Extracellular caspase-6 drives murine inflammatory pain via microglial TNF-α secretion

Temugin Berta,[1] Chul-Kyu Park,[1] Zhen-Zhong Xu,[1] Ruo-Gang Xie,[1] Tong Liu,[1] Ning Lü,[2] Yen-Chin Liu,[2] and Ru-Rong Ji[1,2]

[1]Departments of Anesthesiology and Neurobiology, Duke University Medical Center, Durham, North Carolina, USA.
[2]Pain Research Center, Department of Anesthesiology, Brigham and Women's Hospital, Harvard Medical School, Boston, Massachusetts, USA.

Increasing evidence indicates that the pathogenesis of neuropathic pain is mediated through spinal cord microglia activation. The intracellular protease caspase-6 (CASP6) is known to regulate neuronal apoptosis and axonal degeneration; however, the contribution of microglia and CASP6 in modulating synaptic transmission and pain is unclear. Here, we found that CASP6 is expressed specifically in C-fiber axonal terminals in the superficial spinal cord dorsal horn. Animals exposed to intraplantar formalin or bradykinin injection exhibited CASP6 activation in the dorsal horn. *Casp6*-null mice had normal baseline pain, but impaired inflammatory pain responses. Furthermore, formalin-induced second-phase pain was suppressed by spinal injection of CASP6 inhibitor or CASP6-neutralizing antibody, as well as perisciatic nerve injection of CASP6 siRNA. Recombinant CASP6 (rCASP6) induced marked TNF-α release in microglial cultures, and most microglia within the spinal cord expressed *Tnfa*. Spinal injection of rCASP6 elicited TNF-α production and microglia-dependent pain hypersensitivity. Evaluation of excitatory postsynaptic currents (EPSCs) revealed that rCASP6 rapidly increased synaptic transmission in spinal cord slices via TNF-α release. Interestingly, the microglial inhibitor minocycline suppressed rCASP6 but not TNF-α–induced synaptic potentiation. Finally, rCASP6-activated microglial culture medium increased EPSCs in spinal cord slices via TNF-α. Together, these data suggest that CASP6 released from axonal terminals regulates microglial TNF-α secretion, synaptic plasticity, and inflammatory pain.

Introduction

Tissue injury results in pain hypersensitivity, as a result of peripheral sensitization (sensitization of primary sensory neurons) (1, 2) and central sensitization (sensitization of spinal cord and brain neurons) (3–6). Spinal cord long-term potentiation (LTP) (7, 8) could be regarded as a unique form of central sensitization (3). A growing body of evidence indicates that microglial cells in the spinal cord play an important role in the development of central sensitization and neuropathic pain via neuron-glial interactions (9–14). Peripheral nerve injury induces marked microglial reaction and microgliosis, such as proliferation, morphological changes, and upregulation of microglial markers (e.g., IBA1, CD11b) (14). Nerve injury causes upregulation of the ATP receptor P2X4 and activation of p38 MAPK in spinal cord microglia, which drives neuropathic pain via releasing brain-derived neurotrophic factor (BNDF) (15–18). BDNF was shown to suppress inhibitory synaptic transmission in lamina I spinal cord projection neurons via downregulation of the K^+-Cl^- co-transporter KCC2, impairing Cl^- homeostasis in lamina I neurons (16, 19). Despite a prominent role of microglia in neuropathic pain, there are several outstanding questions regarding how microglia control pain and synaptic transmission.

First, it is not well understood whether microglia can regulate inflammatory pain, in which axonal degeneration and microglial reaction are not so evident (14). In *P2x4*-deficient mice neuropathic pain is blunted, whereas inflammatory pain is only diminished (20). Second, it generally is believed that spinal cord primary afferents release signal molecules (e.g., ATP and chemokines) to activate microglia, but ATP and chemokines (e.g., CCL2) can be released from multiple cell types in the spinal cord, including astrocytes (12, 21). The unique signal molecules from primary afferents as rapid activators of microglia remain to be identified. Finally, spinal cord synaptic plasticity and central sensitization occur within minutes following intense/repetitive C-fiber stimulation (3). Do microglia play a role in acute synaptic plasticity, in the absence of transcriptional regulation?

Caspases are a family of intracellular cysteine proteases and are well known for their roles in regulating apoptosis and neurodegeneration (22). Among different caspases, CASP6 is of particular interest because it is localized in axons and involved in axonal degeneration (23–25). Thus, CASP6 is implicated strongly in Alzheimer's disease (AD) (26, 27). CASP6 activity is associated intimately with AD pathology and memory decline in aged individuals (28). Recent studies also demonstrated a non-apoptotic role of caspases. For example, caspase-3 induces long-term depression and AMPA receptor internalization in hippocampal neurons (29). Caspase-1 and -3 have been implicated in neuropathic pain, by regulating IL-1β and neuronal apoptosis, respectively (30, 31). It is virtually unknown whether CASP6 can modulate synaptic transmission and pain.

Authorship note: Temugin Berta and Chul-Kyu Park contributed equally to this work.

Conflict of interest: The authors have declared that no conflict of interest exists.

Note regarding evaluation of this manuscript: Manuscripts authored by scientists associated with Duke University, The University of North Carolina at Chapel Hill, Duke-NUS, and the Sanford-Burnham Medical Research Institute are handled not by members of the editorial board but rather by the science editors, who consult with selected external editors and reviewers.

Citation for this article: *J Clin Invest.* 2014;124(3):1173–1186. doi:10.1172/JCI72230.

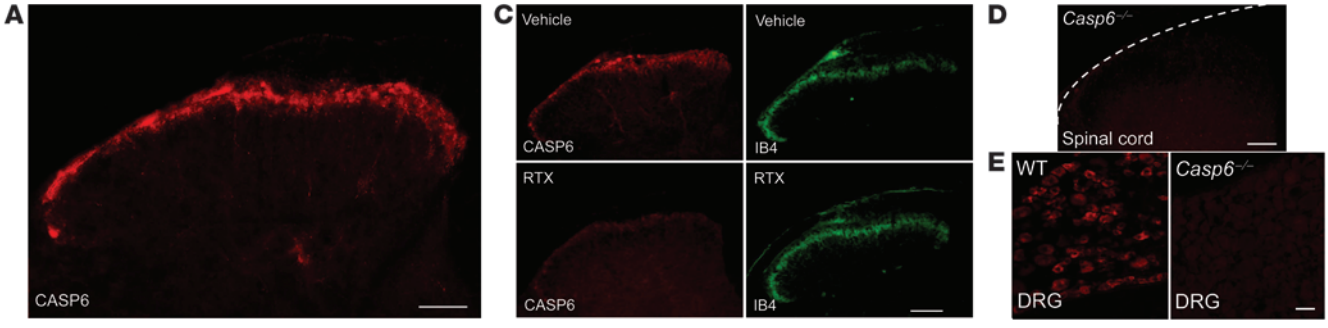

Figure 1
Localization of CASP6 in central terminals of primary afferents in the superficial dorsal horn of the spinal cord. (**A**) CASP6 immunoreactivity in the spinal cord dorsal horn. Scale bar: 100 μm. (**B**) Confocal images of double immunofluorescence showing colocalization of CASP6 and CGRP in axonal terminals of the superficial dorsal horn. Scale bar: 20 μm. (**C**) Ablation of the TRPV1-expressing primary afferents with RTX (10 mg/kg, i.p., daily for 3 days) abolishes CASP6 immunostaining but not IB4 staining in the superficial dorsal horn. Scale bar: 100 μm. (**D**) Absence of CASP6 immunostaining in the dorsal horn of *Casp6*$^{-/-}$ mice. Scale bar: 100 μm. (**E**) CASP6 immunostaining in DRGs of WT and *Casp6*$^{-/-}$ mice. Scale bar: 50 μm.

In this study, we evaluated how extracellular and secreted CASP6 could regulate microglial signaling in inflammatory pain conditions. We found unique localization of CASP6 in spinal cord axonal terminals of C-fiber primary afferents and revealed a non-neurodegenerative role of extracellular CASP6 in pain control. In particular, we demonstrated that extracellular CASP6 could directly modulate spinal cord synaptic transmission and inflammatory pain via releasing TNF-α from microglia. Our findings also suggest an acute action of microglia in regulating synaptic plasticity following noxious stimulation and acute inflammation.

Results

CASP6 is localized in spinal cord central terminals of primary afferents and upregulated after acute inflammation. As a first step to address whether endogenous CASP6 plays a role in pain, we conducted immunohistochemistry to examine CASP6 expression in the spinal cord. Interestingly, we observed CASP6 immunoreactivity only in the superficial dorsal horn (laminae I and II) of the spinal cord, where nociceptive input (unmyelinated C-fibers and myelinated Aδ-fibers) terminates (Figure 1A) (1). Double immunofluorescence revealed colocalization of CASP6 with calcitonin gene–related peptide (CGRP) in axonal terminals (Figure 1B), suggesting that CASP6 is expressed specifically in the central terminals of peptidergic primary afferents.

Transient receptor potential subtype vanilloid-1 (TRPV1) is expressed in peptidergic primary afferents in mouse spinal cord (1). Ablation of the TRPV1-expressing primary afferents with resiniferatoxin (RTX) abolished CASP6 immunostaining but had no effect on IB4 staining in the superficial dorsal horn (Figure 1C). These data support a primary afferent origin of spinal CASP6. CASP6 immunostaining in the spinal cord was absent in *Casp6*$^{-/-}$ mice (Figure 1D), confirming the specificity of the antibody. As expected, CASP6 also was found in small-sized neurons of dorsal root ganglia (DRGs) of WT, but not *Casp6*$^{-/-}$, mice (Figure 1E).

We further examined the regulation of CASP6 in inflammatory pain. Intraplantar injection of diluted formalin (5%) elicited a rapid (within 30 minutes) increase in CASP6 immunoreactivity in CGRP-expressing primary afferents in the medial superficial dorsal horn ipsilateral to the injection (Figure 2A). Interestingly, the primary afferent terminals coexpressing CASP6 and CGRP exhibited close contacts with microglial cell bodies and processes in the spinal cord dorsal horn of *Cx3cr1*-GFP mice, in which all CX3CR1-expressing microglia are labeled with green fluorescence (Figure 2B). Western blot analysis revealed that compared with vehicle, formalin increased the active form of CASP6 (aCASP6, ≈10 and 20 kDa) in the dorsal horn at 30 minutes (Figure 2, C and D), without changing pro-CASP6 (pCASP6, ≈35 kDa, Supplemental Figure 1; supplemental material available online with this article; doi:10.1172/JCI72230DS1). Spinal upregulation of aCASP6 also was induced by intraplantar injection of bradykinin, a well-known inflammatory mediator and pain inducer (Figure 2, C and D). Furthermore, CASP6 levels in CSF were increased significantly after inflammation (Figure 2, E and F), suggesting a possible secretion of CASP6 after inflammation.

Endogenous CASP6 is essential for the genesis of inflammatory pain. We investigated whether pain sensitivity in normal and inflammatory conditions is altered in *Casp6*$^{-/-}$ mice. Compared with WT mice, *Casp6*$^{-/-}$ mice had normal baseline pain, including normal heat pain sensitivity in a tail immersion test (Figure 3A) and normal mechanical pain sensitivity in a Randall-Selitto test (Figure 3B). *Casp6*$^{-/-}$ mice also displayed normal motor coordination in a rotarod test (Figure 3C). Intraplantar formalin injection induced typical biphasic spontaneous pain in WT mice. Notably, the second-phase pain (10–45 minutes), but not the first-phase pain (1–10 minutes), was diminished in *Casp6*$^{-/-}$ mice (Figure 3, D and E). Furthermore, pharmacological inhibition of CASP6 by spinal (intrathecal [i.t.]) injection of the CASP6 inhibitor Z-V-E(OMe)-I-D(OMe)-FMK (ZVEID, 1–10 μg) reduced the second-phase pain in a dose-dependent manner (Figure 3F). Because the peptide inhibitor of CASP6 is cell-permeable and therefore cannot determine

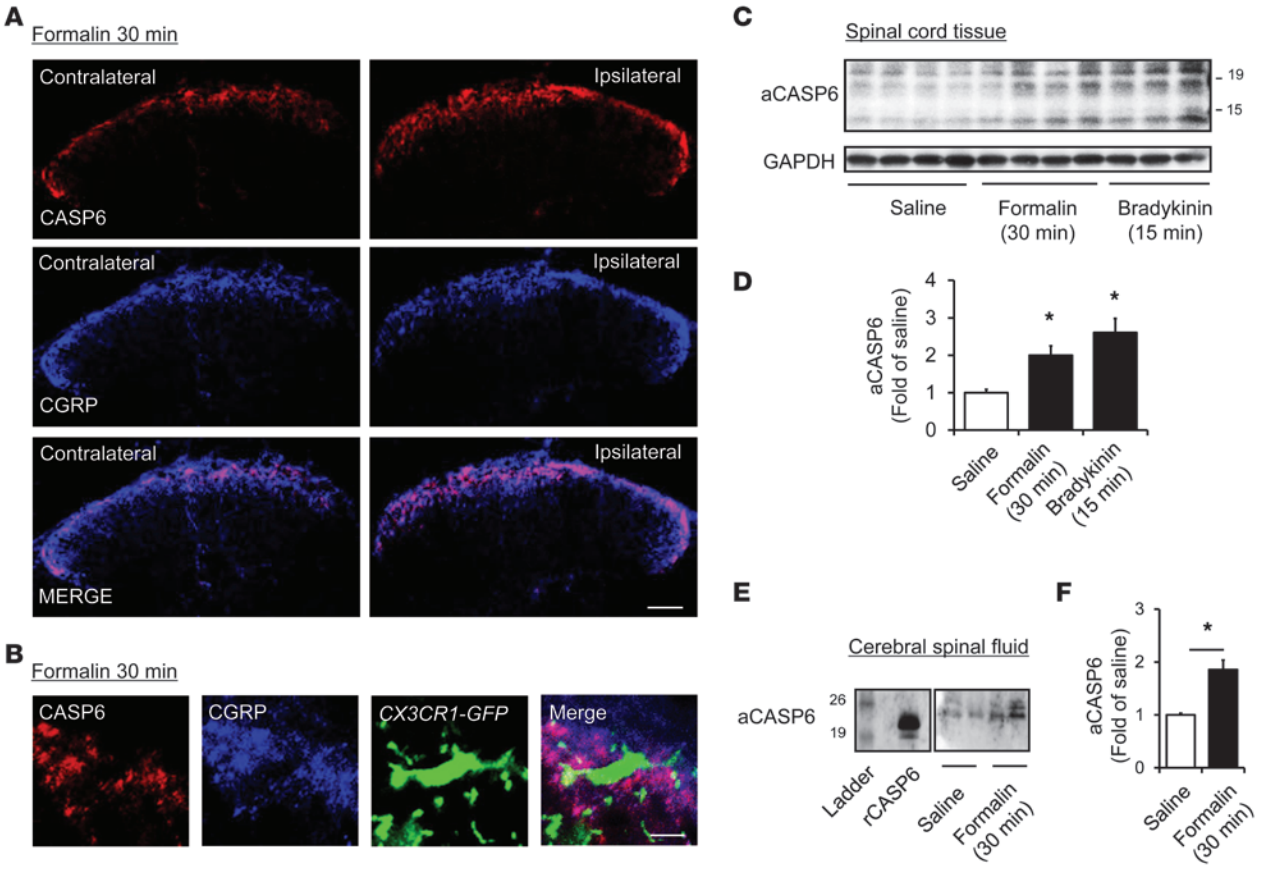

Figure 2

Upregulation of CASP6 in the spinal cord and CSF after acute inflammation. (**A**) Double staining of CASP6 and CGRP in the ipsilateral and contralateral dorsal horn 30 minutes after formalin injection. Scale bar: 100 μm. (**B**) Triple staining of CASP6, CGRP, and CX3CR1 (GFP) in the ipsilateral dorsal horn 30 minutes after formalin injection. Note close contacts between CASP/CGRP-expressing axonal terminals and microglial cell body and processes. Scale bar: 10 μm. (**C** and **D**) Western blot analysis showing the bands of active CASP6 (aCASP6, ≈20 and 10 kDa) 30 minutes after the formalin (5%) injection and 15 minutes after bradykinin (300 ng) injection. (**D**) Intensity of aCASP6 bands. *$P < 0.05$, $n = 3$–4 mice. (**E** and **F**) Western blotting analysis showing increase of aCASP6 in the CSF. The positive control band of rCASP6 is indicated. (**F**) Intensity of aCASP6 bands. *$P < 0.05$, $n = 5$ rats.

the intracellular versus extracellular actions of CASP6, we tested a CASP6-neutralizing antibody that should only target extracellular CASP6. Compared with the control serum, i.t. CASP6-neutralizing antibody specifically reduced the formalin-evoked second-phase pain (Figure 3G). Together, our data suggest an active role of endogenous and extracellular CASP6 in the genesis of acute inflammatory pain.

Given the fact that *Casp6* deletion and spinal CASP6 inhibition only affected the second-phase pain in the formalin test, which is thought to be mediated by spinal cord mechanisms (central sensitization) (3, 32), we postulated that CASP6 induces inflammatory pain via central sensitization. This hypothesis was validated further in the capsaicin test. Intraplantar injection of capsaicin elicited primary and secondary mechanical allodynia in WT mice, but only the secondary mechanical allodynia, which is mediated by central sensitization (33, 34), was attenuated in *Casp6*$^{-/-}$ mice (Supplemental Figure 2, A and B).

Next, we tested whether CASP6 derived from primary afferents would drive inflammatory pain by knocking down CASP6 expression selectively in DRG neurons. To this end, we delivered CASP6-targeting siRNA to the sciatic nerve. Perisciatic injection of fluorescence-labeled siRNA resulted in uptake of siRNA in DRG neurons as a result of axonal transport from the sciatic nerve to DRGs (Supplemental Figure 3A). Notably, siRNA uptake by DRG neurons was potentiated greatly by mixing siRNA with a short peptide derived from rabies virus glycoprotein (RVG-9R) that enables siRNA binding to neurons and enhances knockdown efficiency of siRNA (Supplemental Figure 3B) (35). Perisciatic delivery of CASP6 siRNA, mixed with the RVG peptide, effectively suppressed the formalin-induced second-phase pain (Figure 3H). The siRNA treatment also selectively reduced *Casp6* expression, without affecting the expression of *Casp1* and *Casp3* in DRGs (Figure 3I) and the neuronal injury marker activating transcription factor 3 (*Atf3*) (Supplemental Figure 3C). These results support an active role of CASP6 derived from primary afferent neurons in driving inflammatory pain.

Like capsaicin (36), intraplantar formalin caused degeneration of nerve fibers/axons in the skin as revealed by induction of ATF3 in DRG neurons 3 days after the injection (Supplemental Figure 4), although formalin also was known to induce acute inflammation

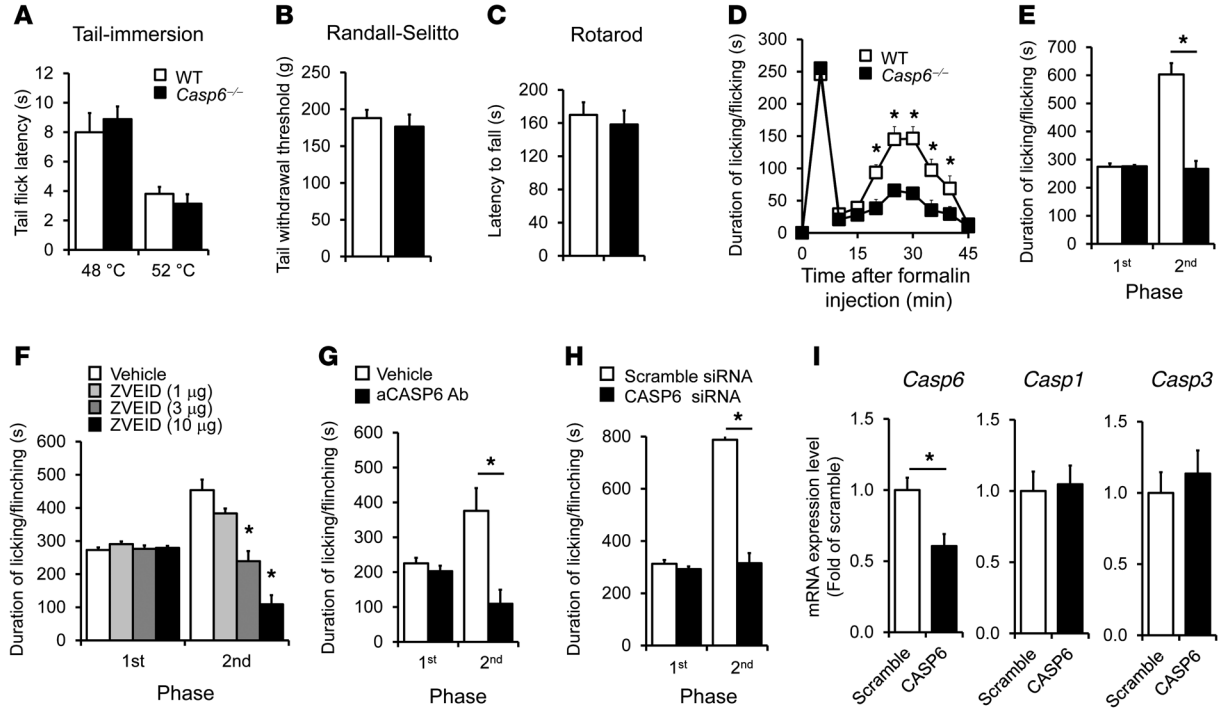

Figure 3

Formalin-induced second-phase inflammatory pain is reduced after deletion of *Casp6*, spinal inhibition of CASP6 with inhibitor or neutralizing antibody, or DRG knockdown of Casp6 with specific siRNA. (**A**–**C**) *Casp6*$^{-/-}$ mice exhibit normal thermal pain (**A**, tail immersion test), mechanical pain (**B**, Randall-Selitto test), and motor function (**C**, rotarod test). $n = 6$ mice. (**D**) Time course (0–45 minutes) of formalin-induced spontaneous pain in WT and *Casp6*$^{-/-}$ mice. $^*P < 0.05$, compared with WT mice, $n = 6$–8 mice. (**E**) Formalin-induced first-phase (1–10 minutes) and second-phase nociceptive responses (10–45 minutes) in WT and *Casp6*$^{-/-}$ mice. $^*P < 0.05$, $n = 6$–8 mice. (**F**) Spinal injection of the CASP6 inhibitor ZVEID (i.t., 1–10 μg) reduces the second-phase pain. $^*P < 0.05$, compared with vehicle (10% DMSO), $n = 5$–6 mice. (**G**) Spinal injection of CASP6-neutralizing antibody (i.t., 1 μg) reduces the second-phase pain. $^*P < 0.05$, $n = 5$–7 mice. (**H** and **I**) Perisciatic delivery of *Casp6* siRNA (2 μg, 6 μl, mixed with the RVG peptide) suppresses the formalin-induced second-phase pain (**H**) and reduces the expression of *Casp6* but not *Casp1* and *Casp3* in DRGs (**I**). Scramble siRNA served as control siRNA. $^*P < 0.05$, $n = 5$–8 mice.

pain via direct activation of TRPA1 (37). To determine a nondegenerative role of CASP6, we tested additional models of acute and persistent inflammatory pain induced by intraplantar injection of irritative chemicals. Bradykinin induced rapid and transient spontaneous pain in WT mice, and this pain in the second phase (5–30 minutes), but not in the initial phase (0–5 minutes), was diminished in *Casp6*$^{-/-}$ mice (Figure 4A). Carrageenan induced persistent mechanical allodynia and heat hyperalgesia for more than 24 hours in WT mice, and both were diminished in *Casp6*$^{-/-}$ mice (Figure 4, B and C). However, carrageenan-induced paw edema was not altered in *Casp6*$^{-/-}$ mice (Figure 4D). CFA produced persistent inflammatory pain for more than 7 days, but *Casp6*$^{-/-}$ mice only showed mild reduction in mechanical allodynia and no reduction in heat hyperalgesia (Figure 4, E and F), possibly because of the compensation of CASP1 and CASP3 in these knockout mice (Supplemental Figure 5). Notably, CASP6 neutralization was still able to reduce CFA-induced allodynia and hyperalgesia in WT, but not in *Casp6*$^{-/-}$, mice (Figure 4, G and H), suggesting a specific role of CASP6 in sustained inflammatory pain, especially mechanical allodynia.

Exogenous CASP6 induces TNF-α release in microglial cultures. To determine the mechanisms by which CASP6 regulates inflammatory pain, we investigated whether and how CASP6 would cause the release of TNF-α, which is synthesized by microglia and contributes to inflammatory pain and central sensitization (38). Stimulation of primary cultures of microglia with recombinant CASP6 (rCASP6, 5 U/ml, 5 U ≈ 0.5 μg) induced a substantial increase (30- to 50-fold) in TNF-α expression (Figure 5A). By contrast, the same treatment did not induce TNF-α expression in primary cultures of astrocytes and DRGs (Figure 5A), indicating that TNF-α is produced primarily by microglia in vitro. rCASP6 also elicited a profound and dose-dependent TNF-α release in microglial culture medium (Figure 5B and Supplemental Figure 6A). This release was dose-dependently inhibited by the CASP6-neutralizing antibody, validating the specificity and efficacy of the antibody (Figure 5C). By comparison, rCASP3 failed to evoke TNF-α release (Supplemental Figure 6B). rCASP6 had mild effects on IL-6 release and no effects on IL-1β release (Figure 5B) and did not cause cell loss of microglia (Supplemental Figure 6, C and D). Western blot analysis revealed that rCASP6 increased the expression of both the membrane-bound TNF-α (precursor, 26 kDa) and the secreted TNF-α (17 kDa), with a much greater increase in secreted TNF-α (Figure 5D and Supplemental Figure 6E), suggesting an important role of rCASP6 in eliciting TNF-α secretion.

We next assessed the signaling transduction pathways involved in the rCASP6-evoked TNF-α release in microglia. rCASP6 induced marked phosphorylation of the MAP kinases ERK and p38

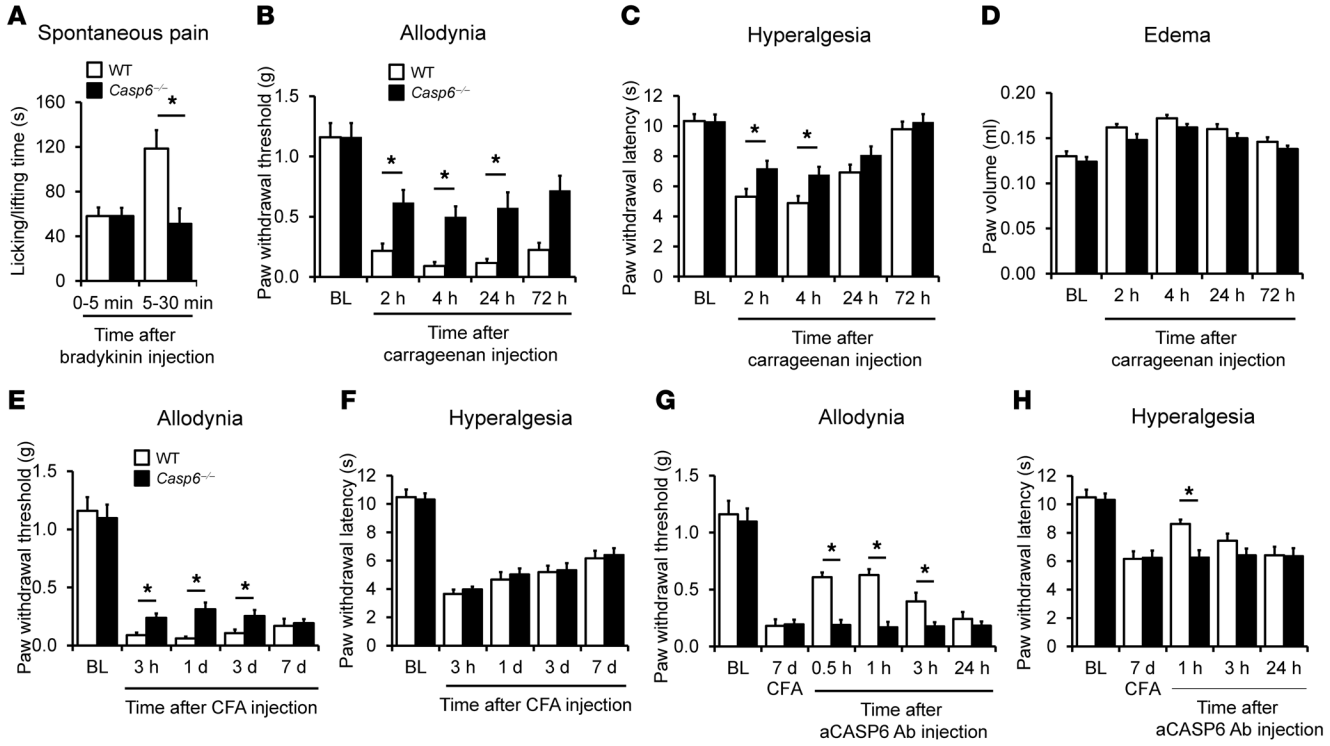

Figure 4

CASP6 contributes to the development of inflammatory pain induced by intraplantar bradykinin, carrageenan, and CFA. (**A**) Bradykinin-induced spontaneous pain in the second phase (5–30 minutes), but not the first phase (0–5 minutes), is reduced in *Casp6*$^{-/-}$ mice. *$P < 0.05$, $n = 7$–8 mice. (**B** and **C**) Carrageenan-induced mechanical allodynia (**B**) and heat hyperalgesia (**C**) are reduced in *Casp6*$^{-/-}$ mice. *$P < 0.05$, compared with WT mice, $n = 5$ mice. (**D**) Carrageenan-induced paw edema (measured as paw volume) is unaltered in *Casp6*$^{-/-}$ mice; $n = 5$ mice. (**E** and **F**) CFA-induced mechanical allodynia (**E**) but not heat hyperalgesia (**F**) is partially and transiently reduced in *Casp6*$^{-/-}$ mice. *$P < 0.05$, compared with WT mice, $n = 5$ mice. (**G** and **H**) Reversal of CFA-induced mechanical allodynia and heat hyperalgesia by CASP6-neutralizing antibody (1 μg, i.t.) in WT mice. *$P < 0.05$, $n = 5$ mice. Note that the CASP6 antibody does not affect inflammatory pain in *Casp6*$^{-/-}$ mice.

(Figure 5D and Supplemental Figure 6E). Treatment of microglia with inhibitor of p38 (SB203580) or ERK kinase (MEK, U0126), but not inhibitors of JNK (SP600125) and PI3K (LY294002), suppressed the rCASP6-induced TNF-α release (Figure 5E), confirming an important role of p38 and ERK in CASP6-triggered TNF-α release. IL-1R–associated kinase-M (IRAK-M) was shown to regulate TNF-α release in leukocytes following CASP6-mediated cleavage (39). rCASP6 also caused cleavage of IRAK-M in microglial cultures (Supplemental Figure 6F). Thus, rCASP6 may trigger TNF-α release via the cleavage of IRAK-M.

TNF-α is expressed by spinal cord microglia and upregulated after acute inflammation. Given the lack of ideal TNF-α antibodies for immunohistochemistry, we conducted single-cell PCR analysis to check *Tnfa* expression in microglia, astrocytes, and neurons in lamina II of spinal cord slices. Figure 6A shows a GFP-labeled microglial cell (CX3CR1^{+}) that was sucked into a glass pipette for single cell analysis. Individual astrocytes also were picked up from *Gfap*-GFP mice. After the reverse transcription, the cDNAs from microglia, astrocytes, and neurons were amplified for 40 and 35 cycles in the first- and second-round PCR, respectively. Notably, the majority of microglia (9 of 10) expressed *Tnfa*. As expected, microglia also expressed the microglial marker *Iba1* (positive control), but not the astrocyte marker *Gfap* (negative control) (Figure 6B). However, astrocytes and neurons did not show positive *Tnfa* bands (Figure 6, C and D). After additional amplification (45 cycles in the second-round PCR), some astrocytes (2 of 5) but not neurons also showed *Tnfa* expression (Figure 6, C and D). Of interest, formalin induced a rapid TNF-α upregulation in the dorsal horn at 30 minutes (Figure 6E), in agreement with a prominent role of this cytokine in the formalin-induced inflammatory pain (38). The formalin-induced upregulation of TNF-α was abolished in *Casp6*$^{-/-}$ mice (Figure 6E).

Exogenous CASP6 induces pain hypersensitivity via microglial and TNF-α signaling. We tested the hypothesis that CASP6 would evoke pain via release of TNF-α. Spinal (i.t.) injection of rCASP6 (5 unit, 5 U ≈ 0.5 μg) elicited rapid (<30 minutes) mechanical allodynia (Figure 7A), and the duration of this allodynia was dose dependent (Supplemental Figure 7A). By contrast, i.t. rCASP3 (5 U) failed to elicit allodynia (Figure 7A), despite CASP3 being implicated in spinal cord neuronal apoptosis and neuropathic pain (30, 31). Thus, extracelluar CASP6 and CASP3 could have distinct bioactivity. Of interest, in double knockout (DKO) mice lacking both TNF receptor type-1 and type-2 (*Tnfr1/2* DKO), the rCASP6-evoked mechanical allodynia was abrogated (Figure 7B). Intrathecal rCASP6 also induced rapid and transient heat hyperalgesia in WT but not *Tnfr1/2* DKO mice (Supplemental Figure 7B). Furthermore, i.t. rCASP6 increased TNF-α expression in the spinal dorsal horn but not in DRGs (Figure 7C).

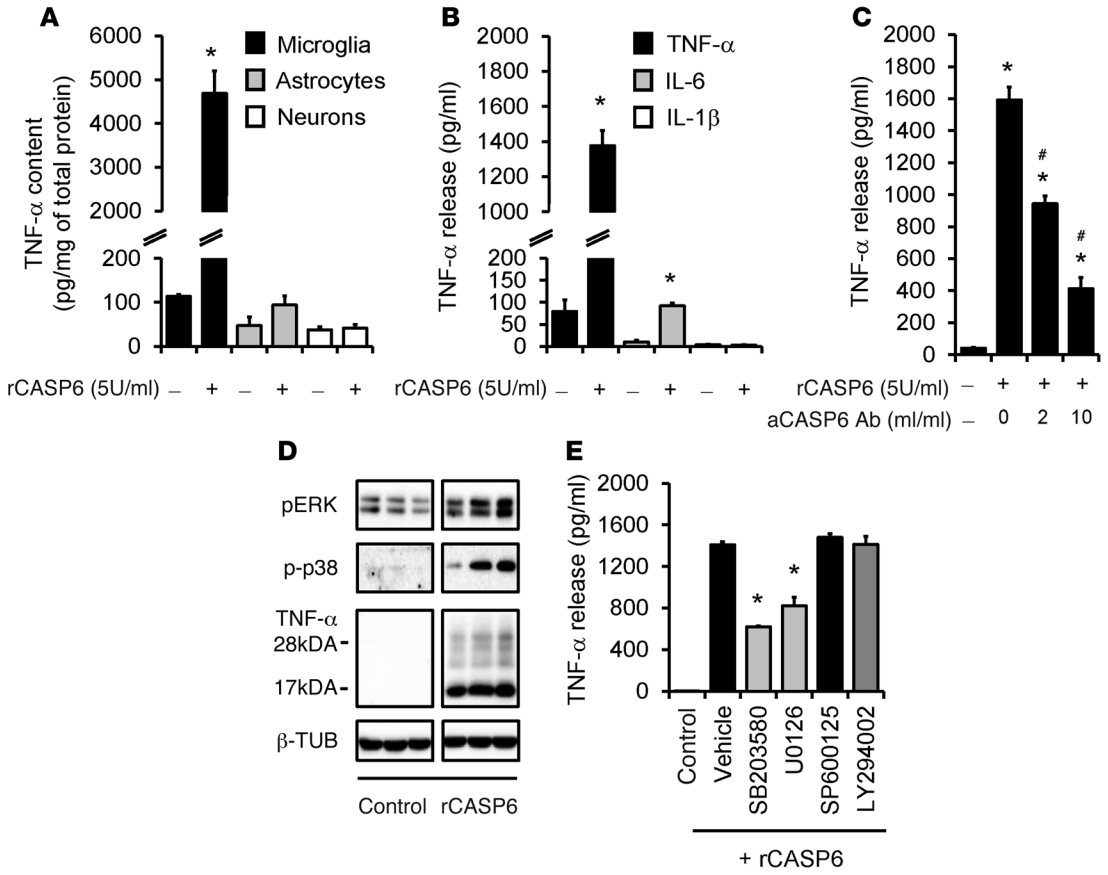

Figure 5

rCASP6 induces TNF-α release in microglial cultures via MAPK activation. (**A**) TNF-α expression, revealed by ELISA analysis, in primary cultures of microglia, astrocytes, and DRG neurons after stimulation of rCASP6 (5 U/ml, 3 hours). *$P < 0.05$, $n = 4$ cultures. (**B**) Release of TNF-α, IL-1β, and IL-6 (ELISA analysis) in microglial culture medium after stimulation of rCASP6 (5 U/ml, 3 hours). *$P < 0.05$, compared with control, $n = 4$ cultures. (**C**) Dose-dependent inhibition of rCASP6-induced (5 U/ml, 3 hours) TNF-α release by CASP6-neutralizing antibody in microglial cultures. *$P < 0.05$, compared with control; #$P < 0.05$; compared with rCASP6, $n = 3$ cultures. (**D**) Expression of pERK, p-p38, and TNF-α, revealed by Western blot analysis, in microglial cultures after rCASP6 (5 U/ml, 3 hours) treatment. All the bands are from the same gel (Supplemental Figure 6E). Note a robust increase in the secreted form of TNF-α (17 kDa). (**E**) Effects of the MAPK inhibitor SB203580, U0126, and SP600125 (50 μM) and the PI3K inhibitor LY294002 (50 μM) on rCASP6-induced TNF-α release in microglial cultures. *$P < 0.05$, compared with vehicle (1% DMSO), $n = 4$ cultures.

Because microglia are a major source of spinal TNF-α (Figure 6B) (40), we examined a possible contribution of spinal microglia to CASP6-evoked allodynia. Pretreatment with minocycline, a microglial inhibitor that has been shown to inhibit neuropathic and postoperative pain (41, 42), reduced the rCASP6-evoked mechanical allodynia (Figure 7D). Intrathecal injection of minocycline, p38 inhibitor, or anti–TNF-α antibody also suppressed the formalin-induced second-phase pain (Supplemental Figure 8, A–C), supporting a role of microglia in acute inflammatory pain. Notably, spinal rCASP6 treatment did not produce signs of axonal degeneration, as we found no loss of peptidergic axons ($CGRP^+$) and non-peptidergic axons labeled with IB4 and thiamine monophosphatase (TMP) in the dorsal horn (Supplemental Figure 9, A–C). By comparison, nerve injury induced a significant loss of axons in the dorsal horn (Supplemental Figure 9D). Collectively, these results indicate that spinal administration of exogenous rCASP6, but not rCASP3, is sufficient to induce pain hypersensitivity via TNF-α and microglial signaling in the absence of neurodegeneration.

Spinal injection of CASP6-activated microglia is sufficient to elicit pain via TNF-α. We examined whether i.t. injection of rCASP6-activated microglia would alter pain sensitivity via TNF-α release. Microglia were stimulated with rCASP6 and then washed three times with PBS and collected for i.t. injection. Compared with nonactivated microglia, injection of rCASP6-activated microglia caused robust mechanical allodynia that lasted for more than 24 hours (Figure 7E), and this allodynia was reduced transiently by i.t. injection of the TNF-α–neutralizing antibody (Figure 7F). Therefore, rCASP6-activated microglia can cause pain hypersensitivity via TNF-α release.

Exogenous CASP6 enhances spinal cord synaptic transmission via TNF-α signaling. To determine the synaptic mechanisms by which CASP6 elicits persistent pain, we recorded spontaneous EPSCs (sEPSCs) in lamina IIo neurons. These neurons are predominantly excitatory, receive input from C-fibers, respond to capsaicin and TNF-α (43), and exhibit marked changes after inflammation (see below). They also form synapses with NK-1–expressing lamina I projection neurons (44), which

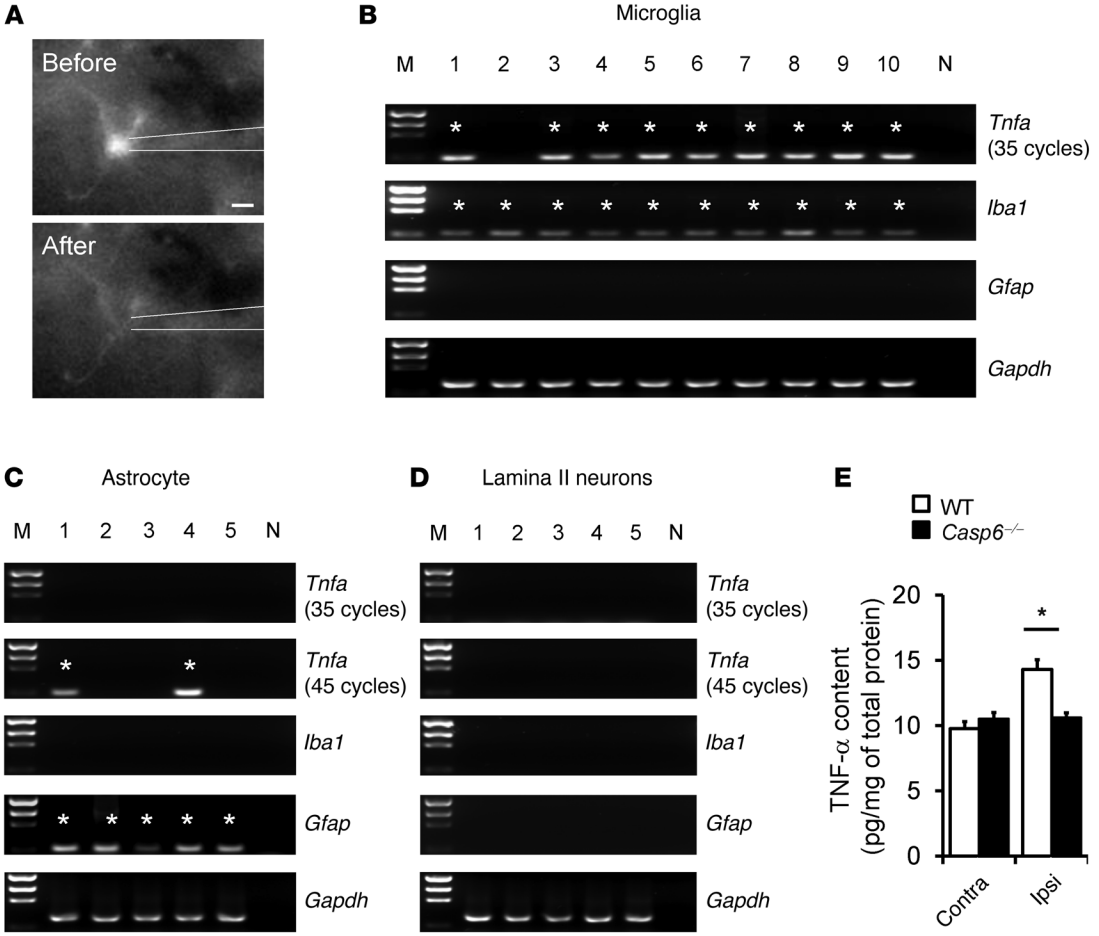

Figure 6

Tnfa is expressed in spinal microglia and upregulated after inflammation. (**A**) A microglial cell is sucked into a glass pipette. Scale bar: 5 μm. (**B**–**D**) Single-cell PCR analysis showing the expression of *Tnfa*, *Iba1*, and *Gfap* in 10 microglia, 5 astrocytes, and 5 neurons in lamina II of spinal cord slices. Note that 90% of microglia express *Tnfa*, and all microglia express *Iba1* but not *Gfap*. Asterisks indicate positive bands. M, markers for DNA sizes; N, negative control; *Gapdh*, positive control. The cDNAs were amplified for 40 and 35 cycles in the first- and second-round PCR, respectively. The *Tnfa* cDNAs from astrocytes and neurons were amplified further for an additional 10 cycles (45 cycles in total) in the second-round PCR. (**E**) ELISA analysis showing TNF-α levels in the ipsilateral (Ipsi) and contralateral (Contra) dorsal horn of WT and *Casp6*$^{-/-}$ mice 30 minutes after the formalin injection. *$P < 0.05$, $n = 6$ mice.

are indispensable for the generation of persistent pain (45). Perfusion of spinal cord slices with rCASP6 (5 U/ml) immediately, within 1 minute, increased the frequency of sEPSCs (Figure 8, A and B). Lamina IIo neurons responded to both rCASP6 and TNF-α by showing increases in the frequency but not the amplitude of sEPSCs (Figure 8, A and B). Consistently, rCASP6 and TNF-α also increased the frequency of miniature EPSCs (mEPSCs) in the presence of 1 μM TTX, and the frequency was increased from 3.3 ± 0.9 to 5.0 ± 0.8 Hz ($P < 0.05$, paired *t* test, $n = 7$ neurons). Together, these results suggest a presynaptic regulation of CASP6 and TNF-α, by releasing glutamate from primary afferent terminals. By comparison, rCASP3 (5 U/ml) had no effects on sEPSC frequency and amplitude (Figure 8C). Importantly, rCAPS6 failed to increase sEPSC frequency in *Tnfr1/2* DKO mice (Figure 8, D and E). rCASP6 and TNF-α further potentiated evoked synaptic transmission (eEPSCs) following electrical stimulation of the dorsal root entry zone in spinal cord slices (Figure 8F).

Endogenous CASP6 contributes to spinal cord synaptic plasticity and LTP following inflammation and tetanic stimulation. Given the importance of spinal cord synaptic plasticity for persistent pain (3), we examined whether endogenous CASP6 would modulate spinal cord synaptic transmission in WT and *Casp6*$^{-/-}$ mice. Neither the frequency nor the amplitude of sEPSCs in lamina II neurons changed in *Casp6*$^{-/-}$ mice (Figure 9, A and B), indicating that CASP6 is not required for basal synaptic transmission in the dorsal horn. Interestingly, CFA inflammation increased the sEPSC frequency in lamina IIo neurons of WT mice, indicating that inflammation-induced synaptic plasticity is retained in spinal cord slices ex vivo. The inflammation-induced sEPSC increases were reduced in *Casp6*$^{-/-}$ mice and also were suppressed by the CASP6 inhibitor ZVEID in WT mice (Figure 9, A and B).

Next, we investigated whether CASP6 plays a role in inducing spinal cord LTP in vivo, which requires TNFR and contributes to persistent pain (7). Tetanic stimulation of the sciatic nerve elicited robust LTP of C-fiber–evoked field potential in the dorsal horn of

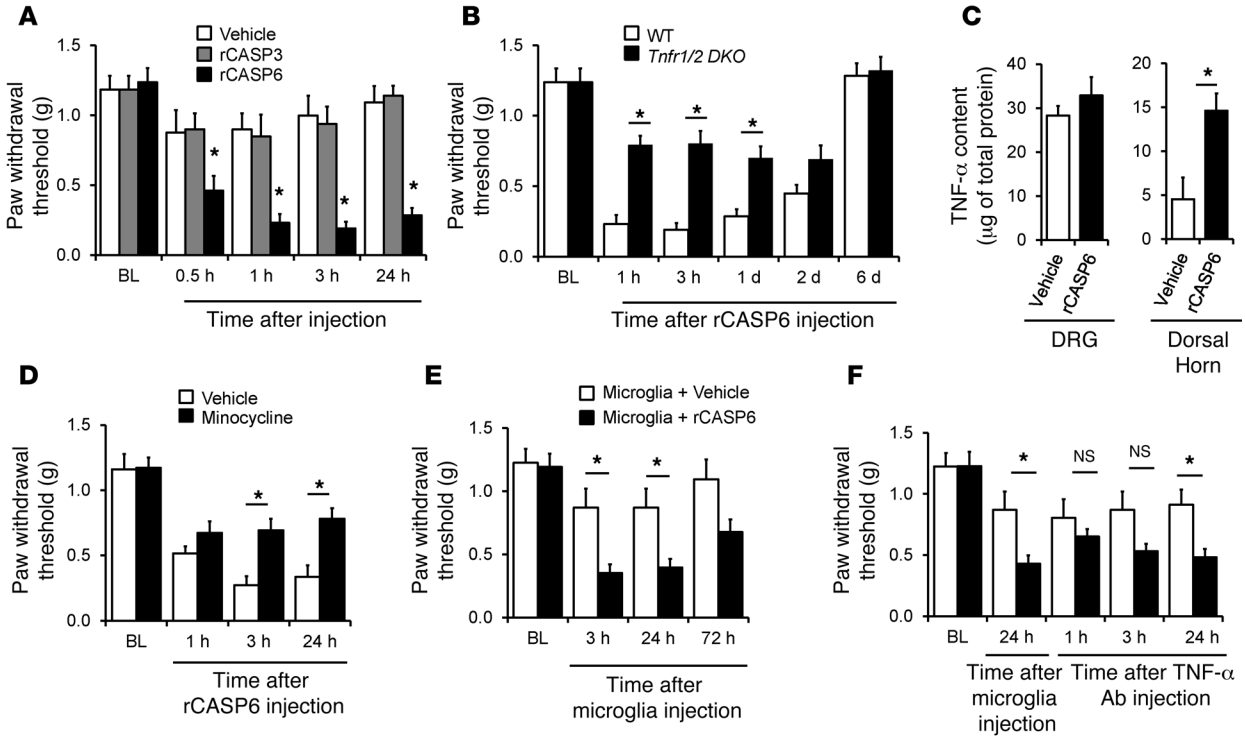

Figure 7

Intrathecal injection of rCASP6 induces mechanical allodynia via microglial and TNF-α signaling. (**A**) Intrathecal rCASP6 but not rCASP3 (5 U) elicits persistent mechanical allodynia. *$P < 0.05$ versus vehicle (PBS), $n = 6–8$ mice. (**B**) rCASP6-induced (i.t., 5 U) mechanical allodynia is abrogated in *Tnfr* double knockout (*Tnfr1/2* DKO) mice. *$P < 0.05$, $n = 7$ mice. (**C**) rCASP6 (i.t., 5 U, 3 hours) increases TNF-α levels in spinal cord but not DRG tissues. *$P < 0.05$, $n = 4$ mice. (**D**) rCASP6-induced (i.t., 5 U) mechanical allodynia is reduced by minocycline pretreatment (i.t., 50 μg). *$P < 0.05$, $n = 5$ mice. (**E**) Spinal (i.t.) injection of rCASP6-stimulated microglia, but not control microglia, induces mechanical allodynia. *$P < 0.05$, $n = 5–7$ mice. (**F**) Transient reversal of mechanical allodynia following injection of rCASP6-stimulated microglia by i.t. TNF-α–neutralizing antibody (5 μg). *$P < 0.05$, $n = 5–7$ mice.

anesthetized WT mice, but not in *Casp6*$^{-/-}$ mice (Figure 9C). Moreover, spinal injection of ZVEID (10 μg, i.t.), given 2 hours after the LTP induction, also reversed spinal LTP (Figure 9D). Thus, CASP6 is required for both the induction and expression/maintenance of spinal LTP. Like *Casp6* deletion, CASP6 inhibition with ZVEID (10 μg/ml ≈ 15 μM) had no effects on baseline sEPSCs (Figure 9E). However, ZVEID partially suppressed the capsaicin-induced sEPSC increases (Figure 9F) and dorsal root stimulation–induced eEPSCs in spinal cord slices (Figure 9, G and H), indicating a unique role of CASP6 in noxious stimulation-induced synaptic activity. ZVEID did not impact sEPSCs and eEPSCs in *Casp6*$^{-/-}$ mice (Figure 9, A, B, G, and H), confirming its selectivity for CASP6.

rCASP6 modulates spinal cord synaptic plasticity via microglial signaling. To determine whether microglial signaling is required for rCASP6-evoked enhancement of synaptic transmission, we treated spinal cord slices with the microglial inhibitor minocycline, at a very low concentration (50 nM), which was shown to block the microglial activator LPS-evoked rapid enhancement (within minutes) in EPSCs in a brain slice without altering basal EPSCs (46). The rCASP6-induced increase in sEPSC frequency was blocked by minocycline (Figure 10, A and B). The capsaicin-induced sEPSC frequency increase also was suppressed by minocycline (Figure 10, A and B). In contrast, minocycline affected neither basal sEPSCs nor a TNF-α–evoked sEPSC frequency increase (Figure 10, A and B). This result suggests that minocycline acts upstream of TNF-α.

We also tested whether minocycline would affect evoked synaptic transmission. Surprisingly, minocycline (50 nM) significantly inhibited a capsaicin-induced sEPSC frequency increase (Figure 10B). In the presence of minocycline, rCASP6 failed to increase the eEPSCs following dorsal root stimulation (Figure 10C). It is likely that persistent activation of C-fibers by capsaicin and dorsal root stimulation could release CASP6 to trigger microglia-mediated synaptic plasticity.

Finally, we evaluated whether rCASP6-activated microglial culture medium would enhance EPSCs. We stimulated microglia with rCASP6 for 3 hours, removed rCASP6 by PBS washing, and collected the fresh culture medium 3 hours later. Exposure of spinal cord slices to the rCASP6-activated microglial culture medium (AMM) was sufficient to increase sEPSC frequency, and this increase by AMM was reversed by the TNF-α–neutralizing antibody (Figure 10, D and E). It is suggested that the rCASP6-activated microglia elicit synaptic plasticity by releasing TNF-α.

Discussion

Caspases were regarded as intracellular proteases that regulate neuronal apoptosis (22). Unlike other caspases, CASP6 is expressed in axons and contributes to axonal degeneration and AD (23–25). We provided several lines of evidence to support an extracellular and non-degenerative role of CASP6 in modulating acute synaptic plasticity and pain hypersensitivity. First, spinal injection of

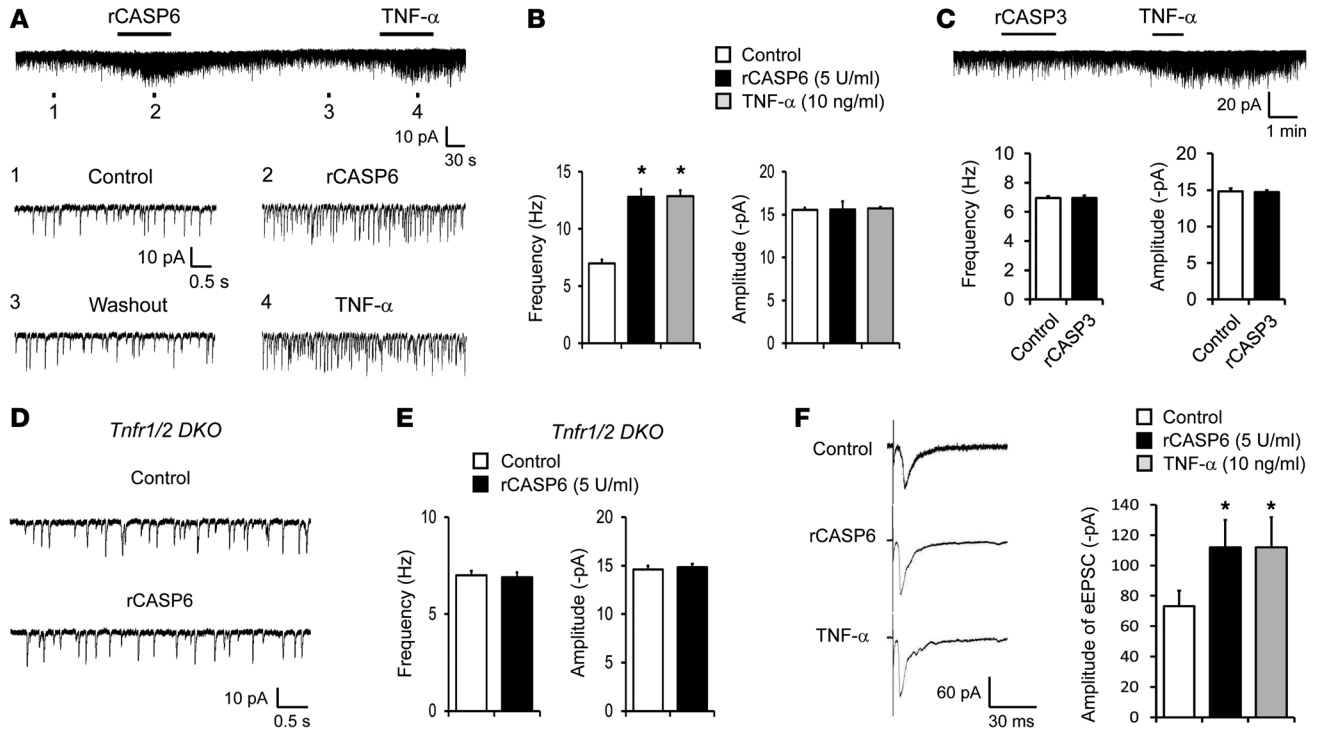

Figure 8

rCASP6 increases EPSCs in lamina IIo neurons of spinal cord slices via TNF-α signaling. (**A**) Traces of sEPSCs in lamina II neurons of spinal cord slices with and without rCASP6 (5 U/ml) and TNF-α (10 ng/ml) incubation. Bottom panels: Enlargement of traces 1–4. Note the same neuron responds to both rCASP6 and TNF-α. (**B**) Frequency and amplitude of sEPSCs as shown in **A**. Note that rCASP6 and TNF-α only increase the sEPSC frequency. **P* < 0.05, *n* = 6–8 neurons. (**C**) Traces of sEPSCs before and after rCASP3 (5 U/ml) and TNF-α (10 ng/ml) incubation. Note that rCASP3 does not change sEPSCs. Bottom panels: Frequency and amplitude of sEPSCs. *n* = 5 neurons. (**D**) Traces of sEPSCs in spinal cord slices of *Tnfr1/2* DKO mice before and after rCASP6 (5 U/ml) incubation. (**E**) Frequency and amplitude of sEPSCs in *Tnfr1/2* DKO mice before and after rCASP6 treatment. Note that rCASP6 does not alter sEPSCs in the DKO mice. *n* = 6 neurons. (**F**) Traces of eEPSCs in lamina IIo neurons of spinal cord slices following dorsal root stimulation before and after TNF-α (10 ng/ml) and rCASP6 (5 U/ml). Amplitude of eEPSCs as fold difference relative to control. **P* < 0.05, *n* = 7–15 neurons.

rCASP6 induced rapid (within 30 minutes) mechanical and thermal pain hypersensitivity without causing axonal degeneration. Second, superfusion of spinal cord slices with rCAPS6 immediately (within 1 minute) increased sEPSC and eEPSC in spinal cord slices. Third, CASP6 is upregulated in the spinal cord dorsal horn and CSF after acute inflammation. Fourth, the secreted CASP6 is essential for the generation of inflammatory pain, because spinal injection of the CASP6 neutralizing antibody effectively blocked formalin and CFA-induced inflammatory pain. Although CASP3 is known to regulate neuropathic pain and long-term depression (29), extracellular rCASP3 failed to elicit pain and modulate sEPSCs, indicating distinct roles of intracellular versus extracellular CASP3. It is conceivable to postulate that rapid nondegenerative actions of rCASP6 may be triggered by extracellular signaling of CASP6, although we should not exclude the well-demonstrated neurodegenerative role of intracellular CASP6 in chronic conditions, such as nerve injury–induced neuropathic pain.

Our results also revealed an acute role of microglial cells in regulating synaptic plasticity and inflammatory pain via possible axonal-microglial interactions (Supplemental Figure 10). CASP6 is specifically localized in CGRP-expressing primary afferent terminals in the superficial dorsal horn and further upregulated in these terminals after inflammation. These central terminals also coexpress the C-fiber marker TRPV1, because CASP6 immunostaining was eliminated completely by the TRPV1 agonist RTX. Further, spinal CASP6 is upregulated in CSF after acute inflammation. Thus, it is conceivable that CASP6 release from axonal terminals serves as a novel activator of microglia in the spinal cord to evoke central sensitization and inflammatory pain. Of interest, central sensitization-driven inflammatory pain, such as formalin- and bradykinin-evoked second-phase spontaneous pain and capsaicin-elicited secondary mechanical allodynia, was reduced in *Casp6*$^{-/-}$ mice. In parallel, minocycline not only inhibited the formalin-induced second-phase pain but also suppressed i.t. rCASP6-induced allodynia and hyperalgesia. Interestingly, rCASP6-induced spinal synaptic changes in both sEPSCs and eEPSCs largely were blocked by minocycline, which also was shown to block EPSC increases following LPS-induced microglial activation in brain slices (46). To further confirm that rCASP6 increases synaptic transmission via microglial signaling, we demonstrated that the culture medium of rCASP6-stimulated microglia was sufficient to increase sEPSCs. This synaptic modulation by CASP6 also was paralleled with behavioral change: spinal injection of rCASP6-activated microglia produced robust pain hypersensitivity.

Mechanistically, we identified TNF-α, which is produced by the majority (90%) of spinal cord microglia, as a key microglial

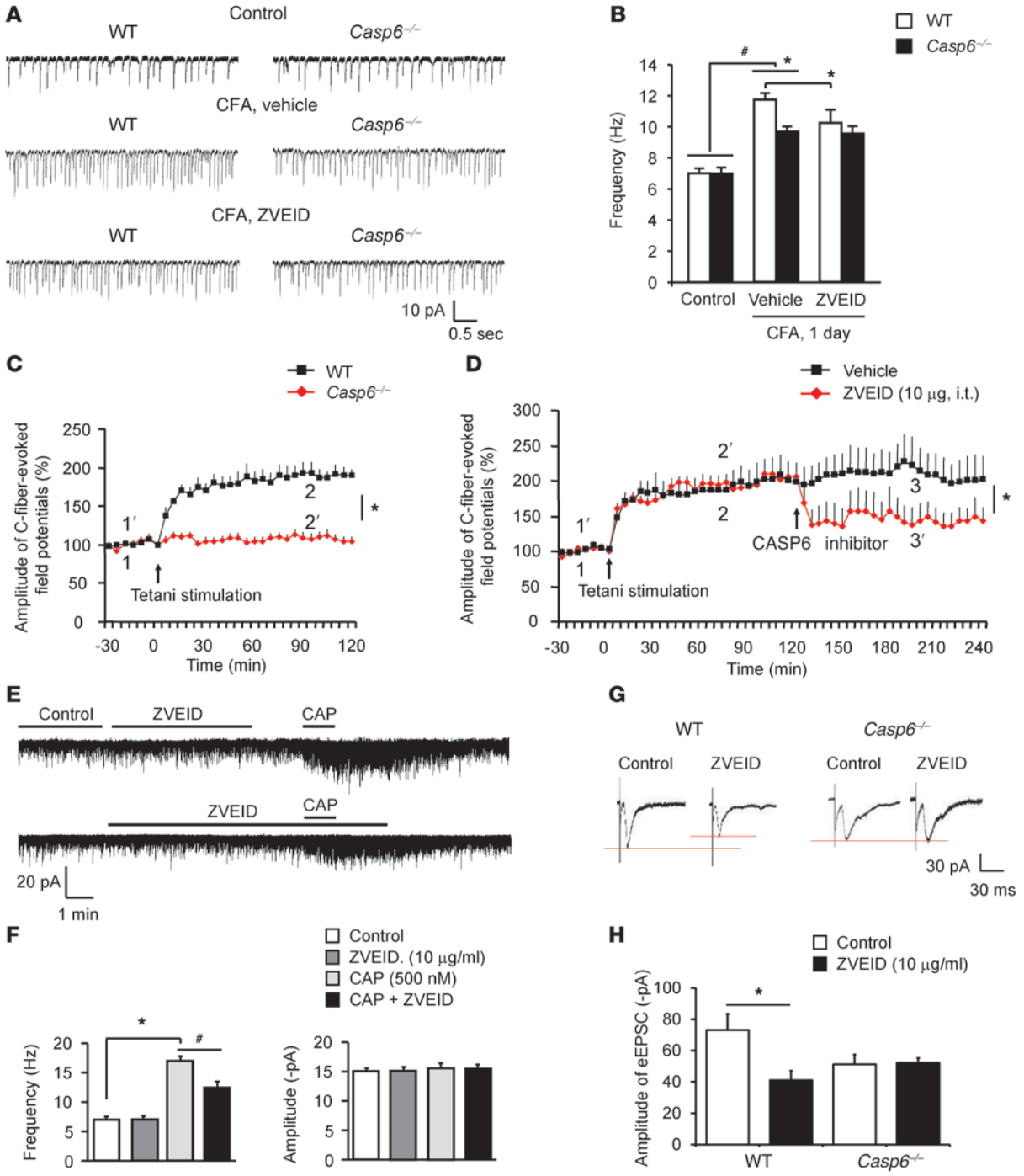

Figure 9

Endogenous CASP6 is essential for inducing spinal cord synaptic plasticity in spinal cord slices and LTP in spinal cord of anesthetized mice. (**A**) Traces of sEPSCs in lamina IIo neurons of spinal cord slices of WT and *Casp6*$^{-/-}$ mice before and after CFA inflammation (1 day). (**B**) Frequency of sEPSCs in WT and *Casp6*$^{-/-}$ mice before and after CFA inflammation and the effects of the CASP6 inhibitor ZVEID. Note the impairment of CFA-induced sEPSC but not the basal sEPSC increases in *Casp6*$^{-/-}$ mice. Also note the inhibition of sEPSCs after CFA inflammation by ZVEID in WT but not *Casp6*$^{-/-}$ mice. *$P < 0.05$, $n = 5$–6 neurons. (**C**) Tetanic stimulation (100 Hz, 1 second, 4 trains, 10 second interval) induces LTP of C-fiber–evoked field potentials in the dorsal horn of anesthetized WT mice but not in *Casp6*$^{-/-}$ mice. *$P < 0.05$ (2-way ANOVA, $n = 5$ mice). (**D**) Reversal of LTP of C-fiber–evoked field potentials in the dorsal horn of anesthetized mice by the CASP6 inhibitor (10 μg, i.t.), administered 2 hours after LTP induction. *$P < 0.05$ (2-way ANOVA, $n = 5$ mice). (**E**) Traces of sEPSCs before and after capsaicin (CAP) treatment (0.5 μM) and the effects of ZVEID (10 μg/ml). (**F**) Frequency and amplitude of sEPSCs recorded in **E**. *$P < 0.05$, $n = 5$–6 neurons. (**G**) Traces of eEPSCs following dorsal root stimulation and the effects of the CASP6 inhibitor in WT and *Casp6*$^{-/-}$ mice. (**H**) Amplitude of eEPSCs. Note that the CASP6 inhibitor loses its effects in *Casp6*$^{-/-}$ mice. *$P < 0.05$, $n = 5$–15 neurons.

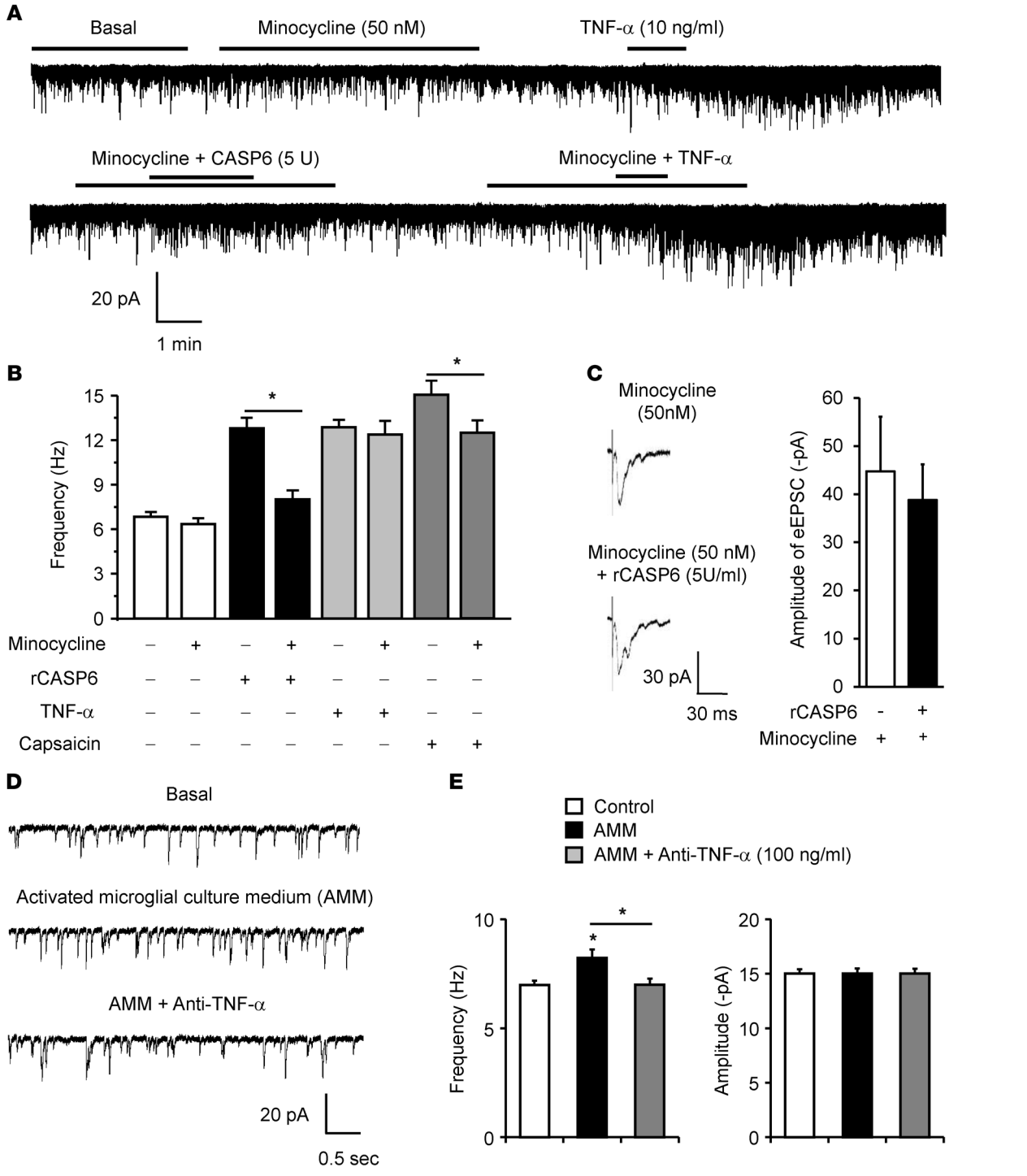

Figure 10

rCASP6 and rCASP6-activated microglia enhance EPSCs in lamina IIo neurons of spinal cord slices via microglial and TNF-α signaling. (**A**) Traces of sEPSCs in lamina IIo neurons of spinal cord slices before and after treatment with rCASP6 (5 U/ml), TNF-α (10 ng/ml), and minocycline (50 nM). (**B**) Frequency of sEPSCs and the effects of rCASP6, TNF-α, capsaicin (0.5 μM), and minocycline. Note that minocycline suppresses the sEPSC increase induced by rCASP6 and capsaicin, but not TNF-α. *$P < 0.05$, $n = 6–8$ neurons. (**C**) Traces of eEPSCs following dorsal root stimulation in the presence of minocycline (50 nM) and minocycline plus rCASP6 (5 U/ml). Right panel: Amplitude of eEPSCs. Note that rCASP6 fails to increase eEPSCs after minocycline treatment. $n = 5$ neurons. (**D**) Traces of sEPSCs following incubation of slices with AMM. The microglial cultures were preactivated by rCASP6 (5 U/ml) for 3 hours and washed with PBS, and the culture medium was collected 3 hours later. Note that the sEPSC frequency increase by AMM is reversed by the TNF-α–neutralizing antibody (1 μg/ml). (**E**) Frequency and amplitude of sEPSC as shown in **E**. *$P < 0.05$, $n = 5$ neurons.

signaling molecule in mediating the effects of CASP6 on synaptic transmission and pain. Strikingly, stimulation of microglia with rCASP6 (but not rCASP3) triggered a substantial release of TNF-α (but not IL-1β), associated with robust upregulation of the secreted 17 kDa TNF-α. Behaviorally, TNF receptors (R1/R2) were essential for the rCASP6-induced mechanical allodynia. TNF-α release also was necessary for eliciting mechanical allodynia following i.t. injection of the rCASP6-activated microglia. In the spinal cord, TNF-α was upregulated after i.t. rCASP6 treatment, and the formalin-induced TNF-α increase was abolished in *Casp6*$^{-/-}$ mice. Together, these lines of evidence reveal TNF-α as a critical microglial mediator to trigger pain hypersensitivity following CASP6-induced microglia activation.

Our data further demonstrated that both exogenous and endogenous CASP6 could modulate acute spinal cord synaptic plasticity via release of TNF-α. Superfusion of spinal cord slices with rCASP6 and TNF-α immediately increased sEPSC frequency in lamina II neurons, and the rCASP6-induced increase was abolished completely in *Tnfr1/2* DKO mice. Our results also suggest that microglia-released TNF-α mediates the effects of CASP6 on synaptic transmission, because a sEPSC increase following stimulation of rCASP6-activated microglial culture medium was reversed by the TNF-α neutralization. Glia-derived TNF-α has been shown to modulate synaptic scaling in cortical neurons (47). How does TNF-α alter synaptic transmission in the spinal cord? We recently demonstrated that TNF-α increased sEPSC frequency via activation of TRPV1 in C-type primary afferent terminals that synapse to lamina IIo excitatory neurons (43), which in turn synapse to lamina I projection neurons (44). Aside from presynaptic effects, TNF-α also acts on postsynaptic dorsal horn neurons to increase the activity of AMPA and NMDA receptors (38, 48). TNF-α also may regulate inhibitory synaptic transmission in the spinal cord via disinhibition (49). TNF-α is required for the induction of spinal LTP and inflammatory pain (43, 50, 51). In addition to direct modulation of synaptic transmission, TNF-α further stimulates glial cells to release proinflammatory mediators to enhance synaptic transmission and LTP (50). Endogenous CASP6 and TNF-α have effects similar to those of exogenous CASP6 and TNF-α on synaptic transmission and inflammation pain. Thus, spinal LTP and inflammatory pain are abrogated after deletion of *Casp6* or *Tnfr* and inhibition of CASP6 and TNF-α (38, 43, 50), and inflammation-induced spinal synaptic plasticity (sEPSC increase) also was impaired by CASP6 inhibition and deletion.

In nerve injury–induced neuropathic pain, microglial BDNF suppresses inhibitory synaptic transmission via transcriptional modulation of KCC2 (16). In inflammatory pain, CASP6-elicited microglial TNF-α could immediately increase excitatory synaptic transmission via translational modulation. The microglial inhibitor minocycline may have nonselective effects on neuronal activity and synaptic transmission at high concentrations (20–100 μM) (50, 52, 53). However, at the low concentration (50 nM) we tested, minocycline does not change basal sEPSCs (46), nor did it affect TNF-α–elicited sEPSC increase (Figure 10, A and B), which argues against direct actions of minocycline on synapses at this very low concentration. Notably, minocycline blocked the rCASP6-elicited changes in sEPSCs and eEPSCs. Furthermore, minocycline inhibited a capsaicin-induced sEPSC increase. Thus, it is possible that C-fiber activation by capsaicin or dorsal root stimulation results in release of CASP6 from primary afferent terminals. Collectively, our findings suggest an active role of microglia in regulating persistently nociceptive activity–induced acute synaptic plasticity via the CASP6/TNF-α pathway (Supplemental Figure 10).

In summary, we revealed what we believe to be a previously unrecognized extracellular role of CASP6 in modulating spinal cord synaptic transmission and inflammatory pain, in sharp contrast to a traditional role of intracellular CASP6 in inducing axonal degeneration and neuronal apoptosis. Based on the unique distribution of CASP6 in spinal cord axonal terminals of C-fibers, we propose a novel form of axonal-microglial interaction in the spinal cord for the induction of inflammatory pain (Supplemental Figure 10). Inflammation causes axonal CASP6 release to trigger TNF-α release from microglial cells, leading to enhanced synaptic transmission and pain states. Both CASP6-induced spinal cord synaptic plasticity and pain hypersensitivity require TNF-α. Future studies are warranted to further the investigation of axonal CASP6 by generating conditional knockout mice to delete CASP6 selectively in nociceptor neurons. Apart from the well-demonstrated chronic role of microglia in regulating neuropathic pain and chronic opioid-induced hyperalgesia (15, 16, 54), we have demonstrated an acute role of microglia in modulating synaptic plasticity and inflammatory/nociceptive pain that occurs after persistent nociceptive input following inflammation or intense noxious stimulation. Thus, targeting the CASP6/TNF-α pathway may offer a new approach for the management of inflammatory pain by modulating rapid changes in spinal cord microglia. Additionally, given the well-known role of CASP6 in axonal degeneration, targeting CASP6 also may alleviate neuropathic pain by protecting against neuropathy.

Methods

Details are provided in the Supplemental Methods.

Reagents. We purchased recombinant full-length active caspase-6 protein (rCASP6) from Abcam and Enzo Life Sciences, rCASP3 from Enzo Life Science, and VEID-fmk (CASP6 inhibitor) and TNF-α from R&D Systems. CASP6- and TNF-α–neutralizing antibodies were obtained from Imgenex and R&D Systems, respectively. Specific siRNA against CASP6 was from Dharmacon, and RVG peptide was synthesized by Invitrogen.

Animals. Knockout mice lacking *Casp6* (*Casp6*$^{-/-}$), *Tnfr1a/1b* (*Tnfr1/2* DKO), *Cx3cr1*/GFP, and *Gfap*/GFP mice, as well as C57BL/6 background WT control mice, were purchased from the Jackson Laboratory. *Casp6*$^{-/-}$ *and Tnfr1/2* DKO mice were viable and showed no developmental defects. Neonatal mice were used to prepare primary cultures of microglia and astrocytes. Young mice (4–7 weeks) were used for electrophysiological studies in spinal cord slices to obtain high-quality recordings. Adult C57BL/6 and CD1 mice (male, 8–10 weeks) were used for behavioral and pharmacological studies. To produce inflammatory pain, diluted capsaicin (1 μg/μl, 5 μl), formalin (5%, 20 μl), bradykinin (300 ng, 10 μl), carrageenan (1.5 %, 20 μl), or CFA (1 mg/ml, 20 μl) was injected into the plantar surface of a hindpaw. For i.t. injection, spinal cord puncture was made with a 30G needle between the L5 and L6 level to deliver reagents (10 μl) to the CSF (55). Adult rats (200–220 g, Charles River) also were used for the CSF collection. For perisciatic injection, Casp6 siRNA (2 μg, 6 μl, mixed with RVG peptide; molar ratio siRNA/RVG = 1:10) or control siRNA (scrambled) was injected 48 hours prior to the behavioral test.

Behavioral testing. Animals were habituated to the testing environment for at least 2 days before the testing. All the behaviors were tested in a blinded manner. We assessed formalin- and bradykinin-evoked spontaneous inflammatory pain by measuring the time (seconds) mice spent licking or flinching the affected paw every 5 minutes for 45 minutes. For testing

mechanical sensitivity, hindpaws were stimulated with a series of von Frey hairs with logarithmically increasing stiffness (0.02–2.56 g, Stoelting), presented perpendicularly to the central plantar surface. Thermal sensitivity was tested using a Hargreaves radiant heat apparatus and expressed as paw withdrawal latency.

Spinal cord slice preparation and patch clamp recordings. As we previously reported (43), the L4–L5 lumbar spinal cord segment was removed from mice under urethane anesthesia (1.5–2.0 g/kg, i.p.) and kept in pre-oxygenated ice-cold Krebs solution. Transverse slices (400–600 μm) were cut on a vibrating microslicer. The slices were perfused with Krebs solution at 36°C for 1–3 hours prior to the experiment. The whole cell patch-clamp recordings were made from lamina IIo neurons in voltage-clamp mode. After establishing the whole-cell configuration, neurons were held at –70 mV to record sEPSCs. mEPSCs were recorded in some neurons in the presence of 1 μM TTX. The resistance of a typical patch pipette is 5–10 MΩ. Membrane currents were amplified with an Axopatch 200B amplifier (Axon Instruments) in voltage-clamp mode. Signals were filtered at 2 kHz and digitized at 5 kHz. Data were stored with a personal computer using pCLAMP 10 software and analyzed with Mini Analysis (Synaptosoft Inc.). To measure eEPSCs in lamina IIo neurons, dorsal root enter zone was stimulated through a concentric bipolar electrode (FHC) with an isolated current stimulator. Test pulses of 0.1 ms with intensity of 3 mA were given at 30 second intervals and monosynaptic C-fiber responses were recorded. Synaptic strength was quantified by the peak amplitudes of eEPSCs. The mean amplitude of 4–5 EPSCs evoked by test stimuli prior to conditioning stimulation served as control.

Spinal cord LTP recordings in anesthetized mice. As we reported previously (43), mice were anesthetized with urethane (1.5 g/kg, i.p.), and a laminectomy was performed at vertebrae T13–L1 to expose the lumbar enlargement. Following electrical stimulation of the sciatic nerve, the field potentials were recorded in the ipsilateral L4–L5 spinal cord segments with glass microelectrodes, 100–300 μm from the surface of the cord. After recording stable responses following test stimuli (2× C-fiber threshold, 0.5 ms, every 5 minutes) for more than 40 minutes, conditioning tetanic stimulation (5× C-fiber threshold, 100 Hz, 1 second duration, 4 trains, and 10 second interval) was delivered to the sciatic nerve for inducing LTP of C-fiber–evoked field potentials. For i.t. drug delivery, a PE5 catheter was inserted via lumbar puncture.

Primary cultures of microglia. Microglia cultures were prepared from cerebral cortexes and spinal cords of 2-day-old postnatal mice. Tissues were then minced into approximately 1 mm pieces, triturated, filtered through a 100 μm nylon screen, and collected by centrifugation at approximately 3,000 *g* for 5 minutes. The cell pellets were dissociated with a pipette and resuspended in medium containing 10% fetal bovine serum in high-glucose DMEM. After trituration, the cells were filtered through a 10 μm screen, plated into T75 flasks, and cultured for 3 weeks. The mixed glia were shaken for 4 hours, and the floating cells were collected and subcultured at a density of 2.5×10^5 cells/ml. After 1 day of plating, the medium was changed to discharge all non-adherent cells. This method resulted in greater than 95% purity of microglia, as assessed by IBA1 and DAPI staining.

Immunohistochemistry. After appropriate survival times, animals were deeply anesthetized with isoflurane and perfused through the ascending aorta with PBS, followed by 4% paraformaldehyde with 1.5% picric acid in 0.16 M phosphate buffer. Spinal cord sections (30 μm, free-floating) and DRG sections (12 μm) were cut in a cryostat and incubated overnight at 4°C with the anti-CASP6 (rabbit, 1:200 to 1:1,000; Cell Signaling Technology) and anti-CGRP (goat, 1:200; Abcam) antibodies, followed by Cy3- or FITC-conjugated secondary antibodies (1:400; Jackson ImmunoResearch Laboratories Inc.) or FITC-conjugated IB4 (10 μg/ml; Sigma-Aldrich). Sections were examined under a Nikon fluorescence microscope and Zeiss confocal microscope.

ELISA. For in vitro experiments, culture medium and cells were collected separately after treatment. For in vivo experiments, animals were transcardially perfused with PBS, and DRG and spinal cord tissues were collected. Cells or tissues were homogenized in a lysis buffer containing protease and phosphatase inhibitors. Protein concentrations were determined by BCA Protein Assay (Pierce). Mouse ELISA kits (TNF-α, IL-1β, and IL-6) were purchased from R&D Systems. For each assay, 50 μg proteins or 50 μl of culture medium were used, and the standard curve was included in each experiment.

Western blot. Protein samples were prepared in the same way as for ELISA analysis, and 20–50 μg of proteins were loaded for each lane and separated by SDS-PAGE gel (4%–15%; Bio-Rad). After the transfer, the blots were incubated overnight at 4°C with polyclonal antibody against total CASP6 (1:1,000, rabbit; Cell Signaling Technology), aCASP6 (active/cleaved, 1:2,000, rabbit; Imgenex), TNF-α (1:500, rabbit; Millipore), p-p38 or pERK (1:500, rabbit; Cell Signaling Technology), and β-tubulin (β-TUB, loading control, 1:5,000, mouse; Millipore) and GAPDH (loading control, 1:10,000, mouse, Millipore). These blots were incubated further with HRP-conjugated secondary antibody and developed in ECL solution. Specific bands were evaluated by apparent molecular sizes. The intensity of the selected bands was analyzed using NIH ImageJ software.

Quantitative real-time RT-PCR. Tissues or cells were isolated rapidly in RNase-free conditions. Total RNAs were extracted using RNeasy Plus Mini kit (QIAGEN). RNAs (0.5–1 μg) were reverse-transcribed using SuperScript III RT (Invitrogen). The sequences of the primers are described in Supplemental Table 1. Quantitative PCR amplification reactions contained the same amount of RT product in a final volume of 15 μl. The thermal cycling conditions comprised 3 minutes of polymerase activation at 95°C, 45 cycles of 10 second denaturation at 95°C, and 30 second annealing and extension at 60°C, and a DNA melting curve was included to test the amplicon specificity.

Single-cell RT-PCR. As previously described (56), single-cell (GFP-labeled microglial cell and astrocyte or non-labeled neuron) in IIo of spinal cord slices was aspirated into a patch pipette with a tip diameter of 5–10 μm, gently put into a reaction tube containing RT reagents, and incubated for 1 hour at 50°C. The cDNA product was used in a separate PCR. The sequences of the outer and inner primers used for single-cell PCR are described in Supplemental Table 2. The first round of PCR was performed in 50 μl of PCR buffer containing 0.2 μM outer primers and amplified for 40 cycles. The reaction was completed with 7 minutes of final elongation. For the second round of amplification, the reaction buffer (20 μl) contained 0.2 μM "inner" primers and 5 μl of the first-round PCR products, which were amplified for 35 cycles and 45 cycles (only for TNF-α cDNAs from microglia and astrocytes). GAPDH was used as a positive control. A negative control was obtained from pipettes that did not harvest any cell contents, but were submerged in the bath solution. The PCR products were displayed on ethidium bromide–stained 1.5% agarose gels.

Statistics. All data were expressed as mean ± SEM. For electrophysiology in spinal cord slices, cells that showed greater than 5% changes from the baseline levels during drug perfusion were regarded as responding ones. We collected the baseline recordings for 2 minutes and the recordings in the first 2 minutes of drug treatment for statistical analysis using paired or unpaired 2-tailed Student's *t* test. LTP data were tested using 2-way ANOVA. Behavioral data were analyzed using Student's *t* test (2 groups) or 1-way ANOVA followed by post-hoc Bonferroni test. The criterion for statistical significance was $P < 0.05$.

Study approval. All the animal procedures were approved by the Institutional Animal Care and Use Committees of Duke University and Harvard Medical School.

Acknowledgments

This study was supported by NIH grants DE17794, DE22743, and NS67686 to R.-R. Ji and NS82985 to Z.Z. Xu. T. Berta was supported by fellowships (PBLAP3-123417 and PA00P3-134165) from Switzerland. Y.C. Liu was supported by a fellowship from the Taiwan National Science Council (97-2918-I-006-012).

Received for publication July 19, 2013, and accepted in revised form December 11, 2013.

Address correspondence to: Ru-Rong Ji, Department of Anesthesiology, Duke University Medical Center, 595 LaSalle Street, GSRB-1, Room 1027A, Durham, North Carolina 27710, USA. Phone: 919.684.9687; Fax: 919.684.2411; E-mail: ru-rong.ji@duke.edu.

1. Basbaum AI, Bautista DM, Scherrer G, Julius D. Cellular and molecular mechanisms of pain. *Cell*. 2009; 139(2):267–284.
2. Hucho T, Levine JD. Signaling pathways in sensitization: toward a nociceptor cell biology. *Neuron*. 2007; 55(3):365–376.
3. Ji RR, Kohno T, Moore KA, Woolf CJ. Central sensitization and LTP: do pain and memory share similar mechanisms? *Trends Neurosci*. 2003;26(12):696–705.
4. Woolf CJ, Salter MW. Neuronal plasticity: increasing the gain in pain. *Science*. 2000;288(5472):1765–1769.
5. Kuner R. Central mechanisms of pathological pain. *Nat Med*. 2010;16(11):1258–1266.
6. Mantyh PW, Hunt SP. Setting the tone: superficial dorsal horn projection neurons regulate pain sensitivity. *Trends Neurosci*. 2004;27(10):582–584.
7. Ruscheweyh R, Wilder-Smith O, Drdla R, Liu XG, Sandkuhler J. Long-term potentiation in spinal nociceptive pathways as a novel target for pain therapy. *Mol Pain*. 2011;7:20.
8. Sandkuhler J. Learning and memory in pain pathways. *Pain*. 2000;88(2):113–118.
9. Ren K, Dubner R. Interactions between the immune and nervous systems in pain. *Nat Med*. 2010;16(11):1267–1276.
10. Tsuda M, Inoue K, Salter MW. Neuropathic pain and spinal microglia: a big problem from molecules in "small" glia. *Trends Neurosci*. 2005;28(2):101–107.
11. Suter MR, Wen YR, Decosterd I, Ji RR. Do glial cells control pain? *Neuron Glia Biol*. 2007;3(3):255–268.
12. McMahon SB, Malcangio M. Current challenges in glia-pain biology. *Neuron*. 2009;64(1):46–54.
13. Milligan ED, Watkins LR. Pathological and protective roles of glia in chronic pain. *Nat Rev Neurosci*. 2009;10(1):23–36.
14. Ji RR, Berta T, Nedergaard M. Glia and pain: is chronic pain a gliopathy? *Pain*. 2013;154(suppl 1).
15. Tsuda M, et al. P2X4 receptors induced in spinal microglia gate tactile allodynia after nerve injury. *Nature*. 2003;424(6950):778–783.
16. Coull JA, et al. BDNF from microglia causes the shift in neuronal anion gradient underlying neuropathic pain. *Nature*. 2005;438(7070):1017–1021.
17. Ji RR, Suter MR. p38 MAPK, microglial signaling, and neuropathic pain. *Mol Pain*. 2007;3:33.
18. Trang T, Beggs S, Wan X, Salter MW. P2X4-receptor-mediated synthesis and release of brain-derived neurotrophic factor in microglia is dependent on calcium and p38-mitogen-activated protein kinase activation. *J Neurosci*. 2009;29(11):3518–3528.
19. Coull JA, et al. Trans-synaptic shift in anion gradient in spinal lamina I neurons as a mechanism of neuropathic pain. *Nature*. 2003; 424(6951):938–942.
20. Tsuda M, Kuboyama K, Inoue T, Nagata K, Tozaki-Saitoh H, Inoue K. Behavioral phenotypes of mice lacking purinergic P2X4 receptors in acute and chronic pain assays. *Mol Pain*. 2009;5:28.
21. Gao YJ, Ji RR. Chemokines, neuronal-glial interactions, and central processing of neuropathic pain. *Pharmacol Ther*. 2010;126(1):56–68.
22. Graham RK, Ehrnhoefer DE, Hayden MR. Caspase-6 and neurodegeneration. *Trends Neurosci*. 2011;34(12):646–656.
23. Nikolaev A, McLaughlin T, O'Leary DD, Tessier-Lavigne M. APP binds DR6 to trigger axon pruning and neuron death via distinct caspases. *Nature*. 2009;457(7232):981–989.
24. Kaplan DR, Miller FD. Neurotrophin signal transduction in the nervous system. *Curr Opin Neurobiol*. 2000;10(3):381–391.
25. Vohra BP, Sasaki Y, Miller BR, Chang J, DiAntonio A, Milbrandt J. Amyloid precursor protein cleavage-dependent and -independent axonal degeneration programs share a common nicotinamide mononucleotide adenylyltransferase 1-sensitive pathway. *J Neurosci*. 2010;30(41):13729–13738.
26. Uribe V, et al. Rescue from excitotoxicity and axonal degeneration accompanied by age-dependent behavioral and neuroanatomical alterations in caspase-6-deficient mice. *Hum Mol Genet*. 2012;21(9):1954–1967.
27. LeBlanc A, Liu H, Goodyer C, Bergeron C, Hammond J. Caspase-6 role in apoptosis of human neurons, amyloidogenesis, and Alzheimer's disease. *J Biol Chem*. 1999;274(33):23426–23436.
28. Ramcharitar J, Afonso VM, Albrecht S, Bennett DA, LeBlanc AC. Caspase-6 activity predicts lower episodic memory ability in aged individuals. *Neurobiol Aging*. 2013;34(7):1815–1824.
29. Li Z, et al. Caspase-3 activation via mitochondria is required for long-term depression and AMPA receptor internalization. *Cell*. 2010;141(5):859–871.
30. Scholz J, et al. Blocking caspase activity prevents transsynaptic neuronal apoptosis and the loss of inhibition in lamina II of the dorsal horn after peripheral nerve injury. *J Neurosci*. 2005;25(32):7317–7323.
31. Joseph EK, Levine JD. Caspase signalling in neuropathic and inflammatory pain in the rat. *Eur J Neurosci*. 2004;20(11):2896–2902.
32. Dickenson AH, Sullivan AF. Peripheral origins and central modulation of subcutaneous formalin-induced activity of rat dorsal horn neurones. *Neurosci Lett*. 1987;83(1–2):207–211.
33. Schwartz ES, et al. Persistent pain is dependent on spinal mitochondrial antioxidant levels. *J Neurosci*. 2009;29(1):159–168.
34. Simone DA, Baumann TK, Collins JG, LaMotte RH. Sensitization of cat dorsal horn neurons to innocuous mechanical stimulation after intradermal injection of capsaicin. *Brain Res*. 1989; 486(1):185–189.
35. Kumar P, et al. Transvascular delivery of small interfering RNA to the central nervous system. *Nature*. 2007;448(7149):39–43.
36. Simone DA, Nolano M, Johnson T, Wendelschafer-Crabb G, Kennedy WR. Intradermal injection of capsaicin in humans produces degeneration and subsequent reinnervation of epidermal nerve fibers: correlation with sensory function. *J Neurosci*. 1998;18(21):8947–8959.
37. McNamara CR, et al. TRPA1 mediates formalin-induced pain. *Proc Natl Acad Sci U S A*. 2007;104(33):13525–13530.
38. Zhang L, Berta T, Xu ZZ, Liu T, Park JY, Ji RR. TNF-α contributes to spinal cord synaptic plasticity and inflammatory pain: distinct role of TNF receptor subtypes 1 and 2. *Pain*. 2011;152(2):419–427.
39. Kobayashi H, et al. Neutrophils activate alveolar macrophages by producing caspase-6-mediated cleavage of IL-1 receptor-associated kinase-M. *J Immunol*. 2011;186(1):403–410.
40. Hanisch UK. Microglia as a source and target of cytokines. *Glia*. 2002;40(2):140–155.
41. Raghavendra V, Tanga F, DeLeo JA. Inhibition of microglial activation attenuates the development but not existing hypersensitivity in a rat model of neuropathy. *J Pharmacol Exp Ther*. 2003; 306(2):624–630.
42. Beggs S, Currie G, Salter MW, Fitzgerald M, Walker SM. Priming of adult pain responses by neonatal pain experience: maintenance by central neuroimmune activity. *Brain*. 2011;135(pt 2):404–417.
43. Park CK, Lu N, Xu ZZ, Liu T, Serhan CN, Ji RR. Resolving TRPV1- and TNF-α-mediated spinal cord synaptic plasticity and inflammatory pain with neuroprotectin D1. *J Neurosci*. 2011;31(42):15072–15085.
44. Todd AJ. Neuronal circuitry for pain processing in the dorsal horn. *Nat Rev Neurosci*. 2010; 11(12):823–836.
45. Mantyh PW, et al. Inhibition of hyperalgesia by ablation of lamina I spinal neurons expressing the substance P receptor. *Science*. 1997;278(5336):275–279.
46. Pascual O, Ben AS, Rostaing P, Triller A, Bessis A. Microglia activation triggers astrocyte-mediated modulation of excitatory neurotransmission. *Proc Natl Acad Sci U S A*. 2012;109(4):E197–E205.
47. Stellwagen D, Malenka RC. Synaptic scaling mediated by glial TNF-α. *Nature*. 2006; 440(7087):1054–1059.
48. Choi JI, Svensson CI, Koehrn FJ, Bhuskute A, Sorkin LS. Peripheral inflammation induces tumor necrosis factor dependent AMPA receptor trafficking and Akt phosphorylation in spinal cord in addition to pain behavior. *Pain*. 2010; 149(2):243–253.
49. Zhang H, Nei H, Dougherty PM. A p38 mitogen-activated protein kinase-dependent mechanism of disinhibition in spinal synaptic transmission induced by tumor necrosis factor-α. *J Neurosci*. 2010; 30(38):12844–12855.
50. Gruber-Schoffnegger D, Drdla-Schutting R, Honigsperger C, Wunderbaldinger G, Gassner M, Sandkuhler J. Induction of thermal hyperalgesia and synaptic long-term potentiation in the spinal cord lamina I by TNF-α and IL-1β is mediated by glial cells. *J Neurosci*. 2013;33(15):6540–6551.
51. Zhong Y, et al. The direction of synaptic plasticity mediated by C-fibers in spinal dorsal horn is decided by Src-family kinases in microglia: the role of tumor necrosis factor-α. *Brain Behav Immun*. 2010;24(6):874–880.
52. Cho IH, et al. Systemic administration of minocycline inhibits formalin-induced inflammatory pain in rat. *Brain Res*. 2006;1072(1):208–214.
53. Zhou LJ, et al. Brain-derived neurotrophic factor contributes to spinal long-term potentiation and mechanical hypersensitivity by activation of spinal microglia in rat. *Brain Behav Immun*. 2011; 25(2):322–334.
54. Ferrini F, et al. Morphine hyperalgesia gated through microglia-mediated disruption of neuronal Cl(–) homeostasis. *Nat Neurosci*. 2013; 16(2):183–192.
55. Kawasaki Y, et al. Distinct roles of matrix metalloproteases in the early- and late-phase development of neuropathic pain. *Nat Med*. 2008;14(3):331–336.
56. Park CK, et al. Substance P sensitizes P2X3 in nociceptive trigeminal neurons. *J Dent Res*. 2010; 89(10):1154–1159.